Available online at www.sciencedirect.com

SciVerse ScienceDirect

Ceramics International 38 (2012) 4901–4908

CERAMICS INTERNATIONAL

www.elsevier.com/locate/ceramint

Characterization of transparent glaze for single-crystalline anorthite porcelain

Xiaosu Cheng, Shanjun Ke *, Qianghong Wang, Hui Wang, Anze Shui, Pingan Liu

College of Materials Science and Engineering, South China University of Technology, 510640 Guangzhou, Guangdong, China

Received 18 January 2012; received in revised form 23 February 2012; accepted 24 February 2012
Available online 5 March 2012

Abstract

The objective of this work was to design a transparent glaze for matching single-crystalline anorthite porcelain. Excessive amounts of quartz were used in glaze to improve surface hardness. Technological properties including hardness and thermal shock resistance were investigated. X-ray diffraction (XRD) and scanning electron microscopy (SEM) studies were also carried out to analyze the microstructure. The phases found in glaze were aluminosilicate glass, quartz and cristobalite crystals. The Vickers hardness of the transparent glaze was about 2.48 GPa, which was much higher than that of commercial soft glaze and was close to hard porcelain glaze due to forming dispersed crystal particles (quartz and cristobalite) in the glass matrix. Moreover, the thermal expansion coefficient of the glaze was slightly lower than that of porcelain body which was easy to produce compressive stress in glaze surface to increase the strength of porcelain. And no cracks were observed on glaze surface after heat exchange three times from 220 °C to 25 °C, presenting excellent thermal shock resistance.

Keywords: Transparent glaze; Microstructure; Hardness; Thermal shock resistance

1. Introduction

Traditionally, porcelain is defined as a glazed or unglazed vitreous ceramic whiteware [1]. With the improvement of living standards people have higher requirements to porcelain tableware, which not only includes high strength for use in automatic dishwashers, but also includes excellent decoration characteristic. As a ceramic material bone china is currently the most upscale tableware product, mainly due to its translucency, whiteness, and high strength [2]. However, bone china is not very suitable in severe service conditions such as hotels and restaurants because its alkaline rich glaze tends to be easily scratched [3]. In addition, bone china has poor thermal shock resistance and does not adapt to the larger changes in temperature. [4,5]. From the result of analysis on the structure of bone china body, the microstructures are known to contain about 30 wt.% anorthite ($CaO{\cdot}Al_2O_3{\cdot}2SiO_2$), 40 wt.% β-tricalcium phosphate (β-$Ca_3(PO_4)_2$) (β-TCP) and 30 wt.% calcium aluminosilicate glass [6,7]. The thermal expansion coefficient (TEC) of anorthite [4] from 20 to 500 °C is ~$4.3 \times 10^{-6}\ K^{-1}$. The TEC for glass [5] of the compositions detected in bone china from 20 to 350 °C is calculated to be 3–$4.5 \times 10^{-6}\ K^{-1}$, while the approximate TEC of β-TCP [5] from 50 to 400 °C is $12 \times 10^{-6}\ K^{-1}$. So, β-TCP crystalline phase should have a negative effect on thermostability for bone china. Meanwhile, anorthite has a refractive index of ~1.58 [8], which is close to that of glass phase at ~1.5 [9]. Thus, properly increase the content of anorthite crystalline phase is beneficial to improve translucency performance of bone china.

In order to design a kind of new porcelain, whose properties fulfill tableware market requirements such as high whiteness, translucency, high strength and low thermal expansion coefficient, anorthite-based porcelain [7,9–12] was considered. It was designed to develop basically anorthite crystals in the microstructure and a high crystalline to glassy phase ratio. Capoglu [9] designed a low-clay translucent whiteware, which consisted of anorthite and mullite ($3Al_2O_3{\cdot}2SiO_2$) crystalline phases. Capoglu and Ustundag [7,12] investigated the mechanical behavior of the low-clay translucent whiteware with different slip's solid content. It was found that the maximum flexural strength was ~135 MPa, when the solid content reached 45 vol.%. However, the production cost was

* Corresponding author. Tel.: +86 20 87114217; fax: +86 20 87110273.
E-mail address: sjkescut@163.com (S. Ke).

0272-8842/$36.00
doi:10.1016/j.ceramint.2012.02.081

much higher than that of bone china bodies due to the need for the prefired materials, which were fabricated by highly pure chemical raw materials at 1370 °C. Mineral materials have been extensively used for ceramics starting compositions. Taskiran and Capoglu [13,14] reported a new porcelainised stoneware material based on anorthite, which was obtained from a mixture of wollastonite, alumina, quartz, magnesia and ball clay by powder pressing and sintering at 1225 °C. The material had anorthite as its major phase with corundum, cristobalite and glass as minor phase, which had high whiteness and high-strength. Nonetheless, corundum was the concomitant crystalline phase, which should cause a negative effect on the translucency performance of anorthite ceramics due to high refractive index (~1.76) [15], comparing with anorthite and glassy phases. Thus, increasing the content of anorthite and reducing the other crystalline phases are good for the translucency property of anorthite-based porcelain. The preparation and characterization of the single-crystalline anorthite porcelain bodies were carried out in detail in a previous study [16].

On the other hand, bone china is defined as soft porcelain, which is first fired in the region of 1220–1250 °C till to full densification [17] and then the glaze applied and fired at around 1050 °C under the condition of a different heating cycle [11]. So, bone china only adapted to a series of low melting glazes including lead and leadless glazes. As a result of stringent lead release limits, the tableware industry prohibited to use lead and moved towards the use of leadless glaze systems such as advanced borosilicate glazes, low and high bismuth glazes and zinc-strontium glazes [18–21]. However, these types of glazes had poor surface hardness which limited their application such as daily domestic use in restaurants and hotels [3,22]. Inversely, hard glaze could be scratch resistant and chemically durable due to high silica content. But such a glaze required a high firing temperature about 1350 °C and had a low thermal expansion coefficient [11]. Furthermore, on the basis of ''Matrix Reinforcement Hypothesis'' [23], the difference in thermal expansion coefficients between the matrix (glassy phase) and dispersed particles (such as quartz and alumina) or crystalline phases formed during firing (such as mullite and cristobalite) produces strong compressive stresses on the glassy phase. Such induced compressive stresses lead to strength improvements in the porcelain bodies [23–26]. In the same way, the theory was applied to porcelain glazes to improve surface hardness in this work. The purpose of this study was to design a transparent glaze for the single-crystalline anorthite porcelain, which comprised a small amount of quartz and cristobalite distributed in the glassy phase. Properties including the phase composition, microstructure, hardness and thermal shock resistance were investigated and reported in detail.

2. Experimental procedure

2.1. Raw materials

Clay A, clay B, quartz, calcite, feldspar and calcined talcum were mineral raw materials and were purchased from Guangdong Sitong Group Co. Ltd. (Chaozhou, China). Calcined alumina, ≥99.0 wt.%, and zinc oxide, ≥99.5 wt.%, were purchased from Hangzhou Wanjing New Material Co. Ltd., China. The chemical compositions of raw materials are shown in Table 1.

2.2. Body preparation

This work was divided into two steps including body preparation and glaze preparation. The raw materials used for porcelain bodies were clay A, quartz, calcite, feldspar and calcined alumina, and the preparation method and process have been elaborated in a previous literature [16]. The XRF chemical analysis result of the single-crystalline anorthite porcelain body is given in Table 2. The phases are anorthite being the only crystalline phase and glass as minor phase (Fig. 1). Fig. 2 shows the high content of porcelain body (etched by 2% HF solution). Clearly, characteristic cuboid or lamellar crystals of anorthite are seen and the average grain sizes are less than 3 μm.

2.3. Glaze preparation

Clay B, quartz, calcite, feldspar, calcined talcum and zinc oxide were used as raw materials in the transparent glazes. Earlier study [23] indicated that, in a porcelain body with excess quartz, the cristobalite phase began to form when the rate of transition of quartz to cristobalite exceeded the rate of quartz dissolution. In order to generate residual quartz and cristobalite crystalline phase in the microstructure, the content

Table 1
Chemical composition of raw materials.

Raw materials	Constituents (wt.%)									
	SiO_2	Al_2O_3	Fe_2O_3	TiO_2	CaO	MgO	ZnO	K_2O	Na_2O	I.L.[a]
Clay A	48.61	36.14	0.21	0.14	0.16	0.21	–	0.98	0.24	12.70
Clay B	53.35	32.27	0.16	0.03	0.28	0.22	–	3.77	0.21	9.58
Quartz	98.38	1.02	0.03	0.01	0.08	0.02	–	0.07	0.04	0.23
Calcite	3.02	0.61	0.04	0.01	53.98	2.13	–	0.04	0.11	39.82
Alumina	–	≥99.0	–	–	–	–	–	–	–	–
Feldspar	65.56	18.85	0.08	0.02	0.23	0.03	–	12.39	2.28	0.56
Talcum	66.23	0.39	0.07	0.02	1.09	31.45	–	0.03	0.01	0.64
Zinc oxide	–	–	–	–	–	–	≥99.5	–	–	–

[a] I.L., ignition loss.

Table 2
XRF analysis result of the single-crystalline anorthite porcelain body fired at 1230 °C for 1 h.

Oxides	SiO_2	Al_2O_3	Fe_2O_3	TiO_2	CaO	MgO	K_2O	Na_2O
wt.%	49.60	26.79	0.09	0.03	19.20	0.81	2.89	0.58

Table 3
Chemical composition of investigated glazes.

Sample	Constituents (wt.%)								
	SiO_2	Al_2O_3	Fe_2O_3	TiO_2	CaO	MgO	ZnO	K_2O	Na_2O
1	65.03	13.99	0.09	0.02	8.95	1.41	2.15	7.12	1.28
2	66.79	13.03	0.08	0.02	8.94	1.41	2.15	6.45	1.16
3	68.55	12.06	0.08	0.02	8.93	1.41	2.15	5.79	1.04
4	70.32	11.10	0.08	0.02	8.92	1.41	2.15	5.12	0.92
5	72.08	10.13	0.07	0.02	8.92	1.40	2.15	4.46	0.79
6	73.84	9.17	0.07	0.02	8.91	1.40	2.15	3.79	0.67

of quartz raw material should be excessive. In this study, 10 wt.% clay B, 15 wt.% calcite, 3 wt.% calcined talcum and 2 wt.% zinc oxide were chosen as the invariable composition while the relative content of quartz and feldspar was changed. A series of compositions are designed in Table 3.

After weighing, mixtures were mixed and milled in a planetary mixer with various ratios of zirconia ball millstone for 4 h. After milling operations, prepared glaze slips were sieved by passing through a 400 mesh sieve (USA Standard Series). Glazes were applied onto porcelain green bodies by means of dipping and pouring. And then the specimens were dried in an oven for 2 h at 90 °C. The firing was performed in an electric furnace at 1230 °C for 1 h. Because the porcelain body had the optimum performances in this firing condition [16].

2.4. Measurements and analyses

The thermal analysis of samples was carried out with a thermal analyzer (Netzsch STA 449C, Selb, Germany) from ambient temperature to 1200 °C at a heating rate of 10 °C/min under air atmosphere. Thermal expansion coefficients of body and glaze were measured over the temperature range from 30 to 500 °C by a thermal dilatometer (Netzsch DIL 402EP). A Vickers microhardness tester (Wilson Wolpert Turkon 2100B, Instron, USA) was used to measure the micro hardness of glaze surface by applying a load of 500 g for 10 s. In order to obtain reliable statistical data, at least 10 indentations were made on each sample. Crystalline phases were determined by an X-ray diffractometer (Philips PW-1710, Netherlands) with CuKa radiation. The microstructures of body and glaze were observed by scanning electron microscopy (SEM) (Philips L30FEG, Netherlands) attached with an energy dispersive spectrometer (EDS).

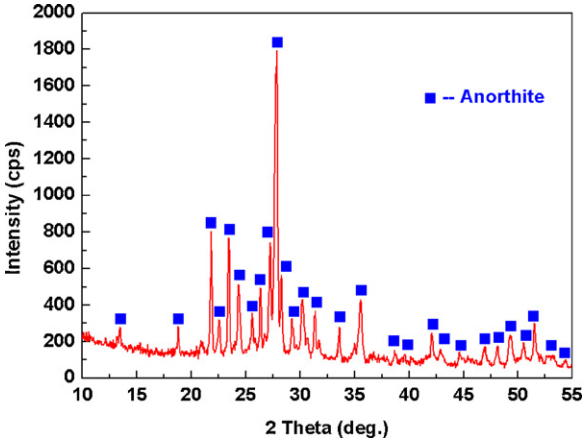

Fig. 1. XRD pattern of the porcelain body fired at 1230 °C for 1 h.

3. Results and discussion

The appearance quality of tableware is crucial for its marketing. In order to obtain a good glaze surface the viscosity and surface tension of glass melt must be considered at high temperature, which are controlled by the ratio between quartz and feldspar in a general way. The results of surface state for different samples are recorded in Table 4. No obvious defect

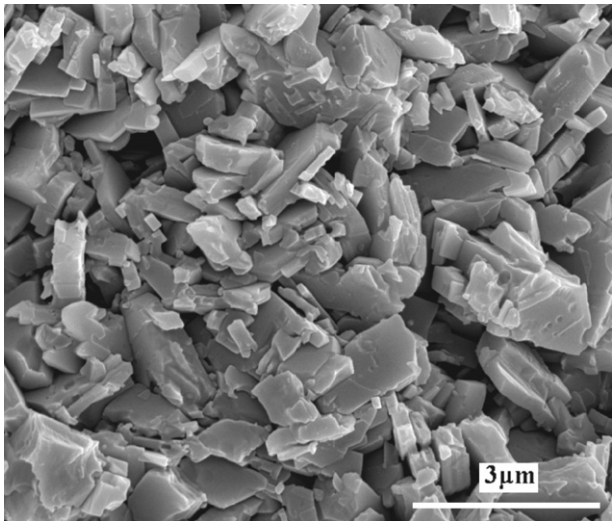

Fig. 2. SEM micrograph of the section of porcelain body fired at 1230 °C for 1 h.

Table 4
Glaze surface quality and quenching experiment results for different samples.

Sample	Glaze surface quality	Number of heat change (220–25 °C)		
		Once	Twice	Three times
1	S	C	–	–
2	S	C	–	–
3	S	N	C	–
4	S	N	C	–
5	S	N	N	N
6	R	–	–	–

S: smooth, R: rough, N: no change, C: cracks on the surface.

was observed on the surface of samples 1–5 while only the surface of sample 6 was not smooth, presenting a small number of pinholes. Because sample 6 is characteristic of high Si, low K and low Na, which is easy to form high viscosity glass melt and causes an unfired glaze surface. According to the concept design for glazes, the investigated glaze should contain a certain amount of quartz and cristobalite. X-ray diffraction (XRD) patterns of samples 4–6 are shown in Fig. 3. The characteristic amorphous hump can be seen within the $2\theta \approx 15$–35° range in samples 4–6, which are associated to a large amount of aluminosilicate glass. Meanwhile, some weak peaks are corresponding to the presence of quartz and cristobalite crystallization. The quartz is likely to be from the starting composition, while the cristobalite phase is crystallized either from the glass phase or by the direct conversion of quartz [23]. Also, the content of quartz and cristobalite increases with increasing ratio of quartz and feldspar.

Thermal shock resistance of tableware is another important factor when considering the thermal matching between glaze and body [27]. There are two evaluations of the thermal shock resistance of porcelain using heating and water-quenching assessment [28]. One is an estimation of the failure criterion by visual determination of crack formation using liquid dye. The other is an estimation of bending strength degradation after the above assessments. In this study, the former was adopted because of its simplicity. The same dimensions test bars were used for the quench experiment from the oven held at 220 °C

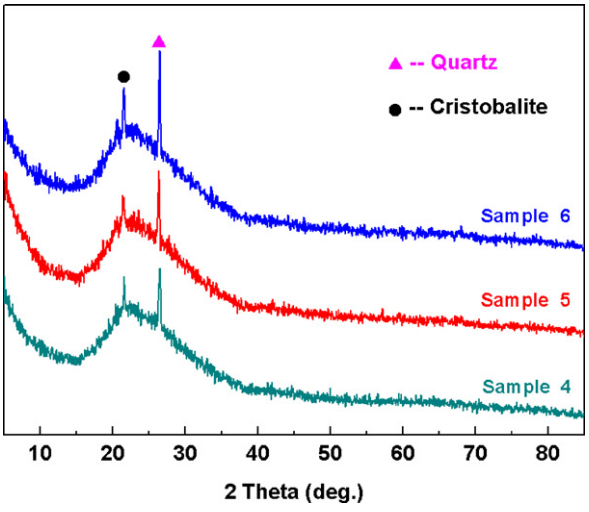

Fig. 3. XRD patterns of samples 4–6 fired at 1230 °C for 1 h.

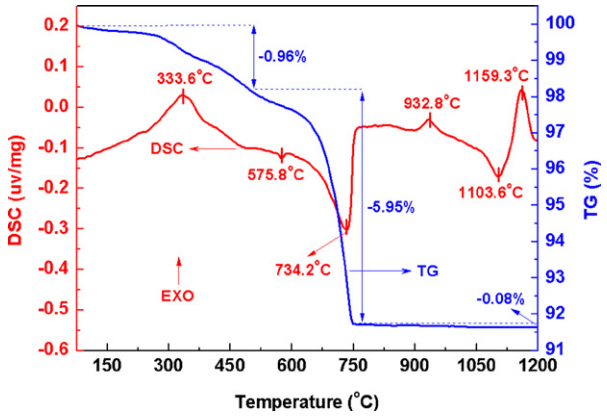

Fig. 4. DSC–TG curves of investigated glaze.

into water held at 25 °C, repeatedly. The results for samples 1–5 are shown in Table 4. The samples 1 and 2 appeared cracks on their surface after heat exchange between 220 and 25 °C once. And no cracks were observed on the surface of specimen 5 upon coloring with dye, heat exchange three times within a temperature difference of 195 °C. The temperature difference of 195 °C is sufficient to withstand the thermal shock in actual use. Hence, the final glaze composition was fixed for sample 5.

Thermo gravimetric (TG) analysis and differential scanning calorimetry (DSC) analysis are used to study weight change and all the transformations during a heating cycle. The TG–DSC curves of the investigated glaze are presented in Fig. 4. An initial weight loss of 0.96 wt.% is observed in the TG curve which is attributable to the removal of residual water and the combustion of the organic matter (333.6 °C). And then, a small endothermic peak at about 575.8 °C is attributed to α- to β-quartz transition. At higher temperatures, the endothermic peak at about 734.2 °C, accompanied by mass loss (5.95 wt.%), which is corresponding to the decomposition of calcite. Meanwhile, there are two exothermic peaks at 932.8 °C and 1159.3 °C, respectively, without weight loss. For the former, some workers attributed this reaction to spinel formation while others attributed it to mullite nucleation [29]. Earlier research [30] suggested that the Si–Al spinel-type structure was transformed by metakaolin at about 950 °C, which was a nonequilibrium unstable phase, certainly transformed to mullite above 1075 °C. Furthermore, additional work on mullite indicated that chemical homogeneity was essential to the formation of mullite at lower temperatures and mullite formation could start at 980 °C [31]. Meanwhile, mullite is a stable phase under high temperature up to 1300 °C [32]. But no mullite was identified through XRD analysis result (Fig. 3). So, this exothermic peak was assigned to the formation of gehlenite ($Ca_2Al_2SiO_7$) in this work, in accordance with the ternary diagram SiO_2–Al_2O_3–CaO [33]. Traore [34] also considered that the gehlenite intermediate phase was crystallised from metakaolinite and calcium at 933 °C, which could transform anorthite at a higher temperature when both SiO_2 and Al_2O_3 were excess. But, from the chemical composition of sample 5 (Table 3), the content of Al_2O_3 was insufficient. On the other hand, the K^+ and Na^+ in the glass matrix, which decreased the viscosity of the glass phase and led to the dissolution of

Table 5
Vickers hardness of traditional soft and hard porcelain glazes and investigated glaze.

Type of glaze	Temperature (°C)	Firing process	Load (kg)	Vickers hardness (GPa)
Soft porcelain glaze	950–1150	Double firing	0.5	0.45–0.74
Hard porcelain glaze	1350–1400	Single firing	0.5	1.7–3.0
Investigated glaze	1230	Single firing	0.5	2.48 ± 0.15

gehlenite at higher temperatures. The latter was due to the formation of cristobalite, indisputably. Lundin [35] has indicated that, in a porcelain body with excess quartz, the cristobalite phase began to form when the rate of transition of quartz to cristobalite exceeded the rate of quartz dissolution.

There is no clear-cut boundary between soft and hard porcelain glaze. Generally speaking, the soft type has a Mohs hardness value of 2–3 and the hard type has a Mohs hardness value of 5–6 [36]. The Vickers hardness commonly is used to quantitative test for hardness in ceramic industry [37]. Consequently, the Vickers micro-hardness of the prepared glaze was also being tested and compared to the other two types of glazes, namely commercial soft and hard porcelain glazes [38]. The results of hardness test are shown in Table 5. As can be seen from Table 5, the Vickers hardness of the investigated glaze is about 2.48 GPa which is far higher than that of soft porcelain glaze and is close to that of hard porcelain glaze.

Previous research [39] indicated that various parameters such as amount and kind of crystalline phases, microstructures and composition of residual glassy phase could affect the hardness of a porcelain glaze. Fig. 5 shows the SEM micrographs of the investigated glaze surface, etched by 2% HF solution. Clearly, a large number of crystals like worms disorderly distribute in glass matrix (Fig. 5a). Fig. 5b shows that porous structures on the surface are presented due to acid treatment. Fig. 5c and d presents two different modalities of crystals, respectively. Also, the chemical composition of crystals was analyzed by EDS in Fig. 6. The result reveals the presence of Si and O, which indicates the same chemical composition for two kinds of crystals. Combining with XRD analysis in Fig. 3, one is the residue quartz which forms a big aggregate (Fig. 5c), the other is nearly spherical cristobalite (Fig. 5d). Zawrah and Hamzawy [40] also fabricated the rounded cristobalite gains from pure alumina and borosilicate glass fired at 1300 °C. The cristobalite grains tend to be much smaller than the quartz grains because of being crystallized either from the glass phase or by the direct conversion of quartz [23]. The higher hardness is attributed to the existence of quartz and cristobalite in the glass matrix. Moreover, Silva [41] has fabricated an opaque glaze by means of zircon formation, and the hardness could reach 3.6 GPa. The addition of fine-grained polycrystalline tetragonal zirconia (3% Y_2O_3–TZP) to conventional ceramic glazes was studied by Llusar [42], and the hardness was enhanced up to 8.4 GPa. However, both of zircon and zirconia are not suitable for using in transparent glaze because of the opaque appearance.

The microstructure of cross-section was carried out using a scanning electron microscopy (Fig. 7). The boundary line between glaze layer and body can be clearly distinguished at higher magnification (Fig. 7a and b). The thickness of glaze layer is about 100 μm (Fig. 7a), while the interfacial zone is about 10 μm thick and continuous throughout the interface and

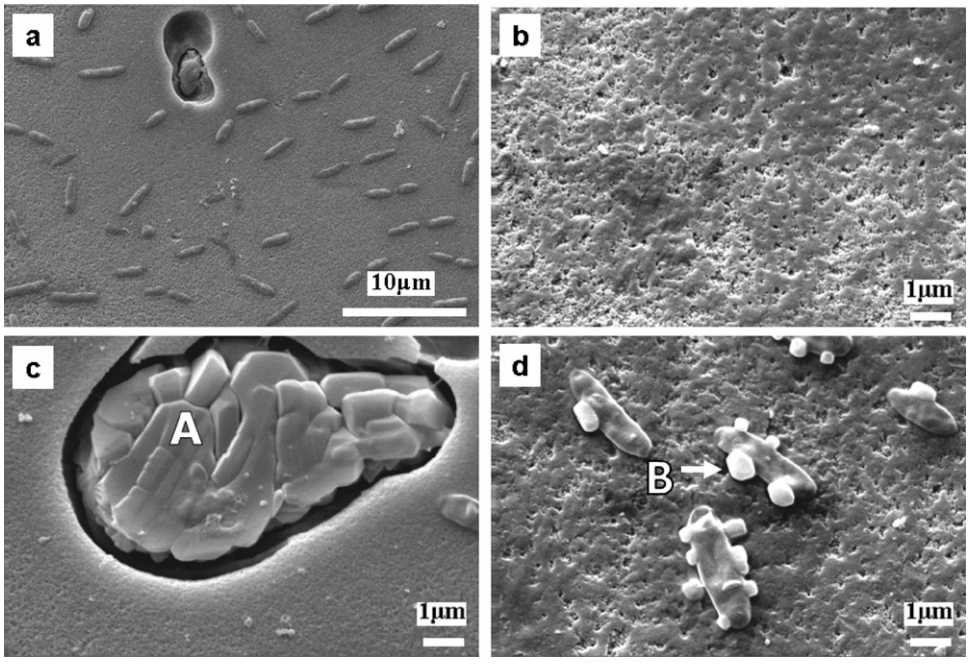

Fig. 5. SEM micrographs of the investigated glaze surface from different regions.

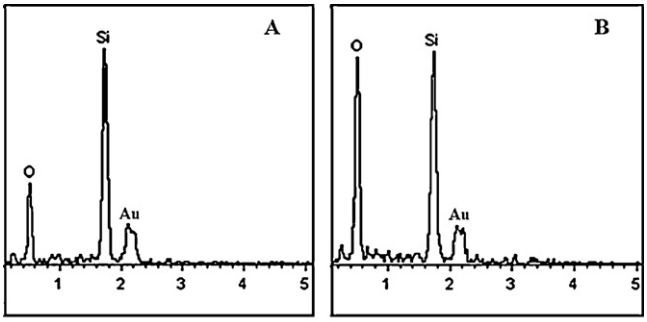

Chemical element	Percentage (wt.%)
O	39.09
Si	60.91

Chemical element	Percentage (wt.%)
O	57.69
Si	42.31

Fig. 6. EDS analysis of the investigated glaze surface by the points labeled (A) and (B) in Fig. 5.

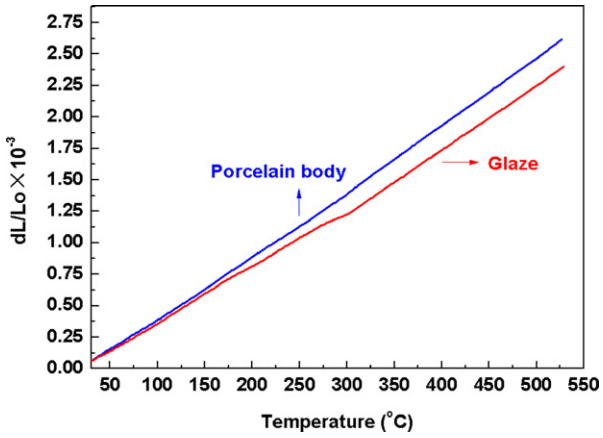

Fig. 8. Thermal-expansion ratio curve of porcelain body and glaze as a function of temperature.

this zone appears to be more highly crystalline than the bulk of glaze layer (Fig. 7c). Also some crystals which had been previously formed in the porcelain body microstructure seem to be continued growing into the glaze contributing for the formation of interfacial zone. Energy dispersive spectra (EDS) from the interfacial zone are given in Fig. 7d. The result reveals the presence of K, Na, Ca, Al, Si and O element, which is similar to the glaze composition. And some grains of the porcelain body also exist in the interfacial zone. From the point of view of thermal expansion mismatch, the presence of the interfacial zone can be beneficial if its coefficient of thermal expansion is to be intermediate between that of the porcelain body and glaze [11].

When glazing a porcelain substrate, it is important to avoid the generation of destructive stresses at the glaze/body interface. Stress in the glaze layer develops as a result of difference in thermal contraction between the glaze and body as they cool from the firing temperature down to room temperature. To prevent excessive and destructive stresses being generated, the thermal expansion coefficient of a glaze should, ideally, be carefully matched with that of ceramic body, so that it should be same or slightly lower. The thermal expansion behavior of the porcelain body and glaze was measured between room temperature and 500 °C as shown in Fig. 8. The expansion ratio of the porcelain body and glaze is almost linear increase, and the expansion ratio of the porcelain body is slightly higher than that of glaze over the entire measured temperature range, which is easy to produce compressive stress in glaze surface to increase the strength of porcelain. Also, Kobayashi [43] reported the bending strength of porcelain was improved from 160 MPa up to 230 MPa by compressive stress in glaze. Moreover, for practical application of high-strength porcelain for tableware, thermal expansion below 150 °C is important in order to

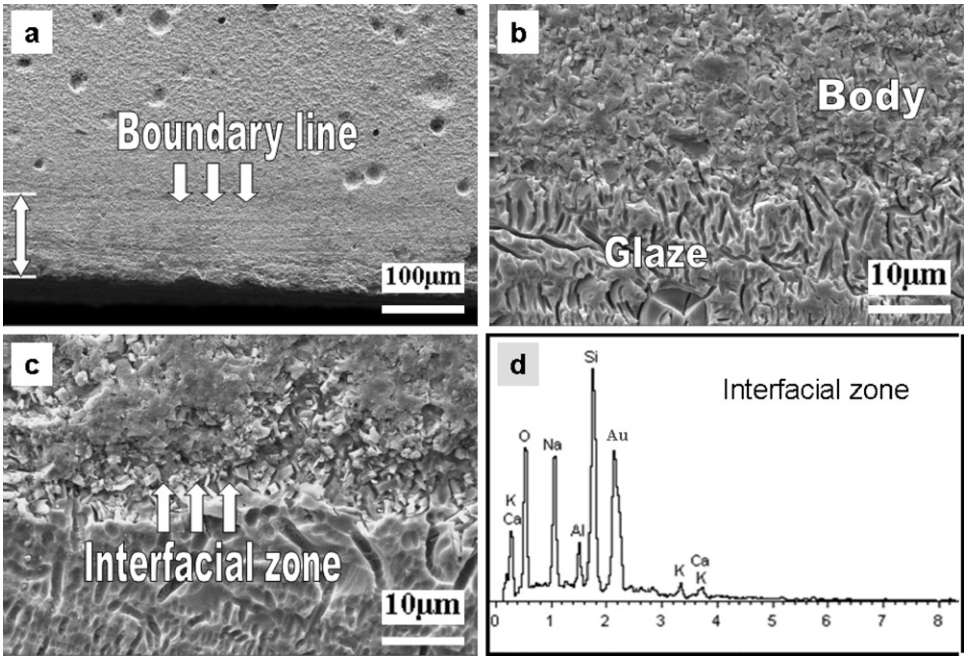

Fig. 7. SEM micrographs of the cross-section of investigated glaze, EDS from interfacial zone.

Table 6
Average TEC of porcelain body and glaze in various ranges of temperature.

Temperature (°C)	Thermal expansion coefficient, α ($\times 10^{-6}$ K^{-1})		
	Porcelain body	Glaze	$\Delta\alpha$
25–100	4.6472	4.0543	+0.5929
25–200	4.8745	4.4525	+0.4220
25–300	4.9142	4.6557	+0.2585
25–400	5.0601	4.8468	+0.2133
25–500	5.1189	5.0546	+0.0643

withstand the thermal shock of heat disinfection or washing [28]. The average TEC values of the porcelain body and glaze in the area of the tested temperature are calculated and listed in Table 6. From the table, the difference in thermal expansion coefficient of body and glaze is positive and remains between 0.06×10^{-6} and 0.59×10^{-6} K^{-1}, which indicates that the investigated glaze can be well matched with the single-crystalline anorthite porcelain body. Consequently, no cracks were observed on the glaze surface after heat exchange three times from 220 °C to 25 °C, presenting high thermal shock resistance.

4. Conclusion

A transparent glaze for matching single-crystalline anorthite porcelain was fabricated and its structure and properties including surface hardness and thermal shock resistance were investigated. It was found that the phases were mostly aluminosilicate glass, a small amount of residual quartz and cristobalite in the transparent glaze and the content of quartz and cristobalite increased with increasing ratio of quartz and feldspar. The surface hardness of the transparent glaze determined by the Vickers hardness was about 2.48 GPa, which was much higher than that of commercial soft glaze and was close to hard porcelain glaze due to forming dispersed crystal particles (quartz and cristobalite) in the glass matrix. What's more, the thermal expansion coefficient of the investigated glaze was slightly lower than that of porcelain body and the difference between them remained between 0.06×10^{-6} and 0.59×10^{-6} K^{-1}, which indicates that the transparent glaze coulld be well matched with the single-crystalline anorthite porcelain body. There were no cracks on the glaze surface after heat exchange three times from 220 °C to 25 °C. So, the transparent glaze was sufficient to withstand the thermal shock in actual use.

Acknowledgements

This work was supported by the Major Scientific and Technological Projects of Guangdong Province (No. 2010A080804001) and the ChanXueYan Special Funds of Guangdong (No. 2011B090400201).

References

[1] Kr.D. Swapan, D. Kausik, Differences in densification behavior of K- and Na-feldspar-containing porcelain bodies, Thermochim. Acta. 406 (2003) 199–206.
[2] A. Kara, R. Stevens, Characterisation of biscuit fired bone china body microstructure. Part I: XRD and SEM of crystalline phases, J. Eur. Ceram. Soc. 22 (2002) 731–736.
[3] A. Capoglu, Elimination of discoloration in reformulated bone china bodies, J. Eur. Ceram. Soc. 25 (2005) 3157–3162.
[4] B. Ryu, I. Yasui, Sintering and crystallization behavior of a glass powder and block with a composition of anorthite and the microstructure dependence of its thermal expansion, J. Mater. Sci. 29 (1994) 3323–3328.
[5] Y. Iqbal, P.F. Messer, W.E. Lee, The non-equilibrium microstructure of bone china, Br. Ceram. Trans. 99 (2000) 110–116.
[6] A. Kara, R. Stevens, Characterisation of biscuit fired bone china body microstructure. Part II: transmission electron microscopy of glassy matrix, J. Eur. Ceram. Soc. 22 (2002) 737–743.
[7] C.B. Ustundag, Y.K. Tur, A. Capoglu, Mechanical behavior of a low-clay translucent whiteware, J. Eur. Ceram. Soc. 26 (2006) 169–177.
[8] D.R. Lide, CRC handbook of chemistry and physics, 72nd ed., CRC Press, Boston, 1992.
[9] A. Capoglu, P.F. Messer, Design and development of a chamotte for use in a low-clay translucent whiteware, J. Eur. Ceram. Soc. 24 (2004) 2067–2072.
[10] A. Capoglu, A novel approach to high-strength, translucent whitewares using prefired materials, Key Eng. Mater. 264-268 (2004) 1585–1588.
[11] A. Capoglu, A novel low-clay translucent whiteware based on anorthite, J. Eur. Ceram. Soc. 31 (2010) 321–329.
[12] A. Capoglu, M.U. Taskiran, Fabrication of low-clay containing translucent whiteware using prefired materials by slips casting, Key Eng. Mater. 264-268 (2004) 1621–1624.
[13] M.U. Taskiran, N. Demirkol, A. Capoglu, A new porcelainised stoneware material based on anorthite, J. Eur. Ceram. Soc. 25 (2005) 293–300.
[14] A. Capoglu, M.U. Taskiran, Processing of ultra white porcelain stoneware based on anorthite, Key Eng. Mater. 264-268 (2004) 1495–1498.
[15] C.B. Carter, M.G. Norton, Interacting with and generating light, Ceram. Mater. Sci. Eng. VII (2007) 575–597.
[16] X.S. Cheng, S.J. Ke, Q.H. Wang, H. Wang, A.Z. Shui, P.A. Liu, Fabrication and characterization of anorthite-based ceramic using mineral raw materials, Ceram. Int. (2011), doi:10.1016/j.ceramint.2011.12.028.
[17] C.E.L. Franklin, A.J. Forrester, The development of bone china parts I and II, Trans. Br. Ceram. Soc. 74 (1975) 141–145.
[18] R.C.P. Cubbon, Consumer and environmental pressures on the use of lead glazes and colors, Interceramics 43 (1994) 240–242.
[19] S. Alsop, Development of unleaded glazes for ceramic tableware, Br. Ceram. Trans. 93 (1994) 77–79.
[20] P.R. Jackson, Unleaded glazes and colors for tableware an update, Br. Ceram. Trans. 94 (1995) 171–173.
[21] A. Kara, R. Stevens, Interactions between an ABS type leadless glaze and a biscuit fired bone china body during glost firing-Part II: investigation of interactions, J. Eur. Ceram. Soc. 22 (2002) 1103–1112.
[22] P.F. Messer, R.J. Hand, S. West, S. Batista, A. Capoglu, M.K. Kiang, Design and development of a low-clay translucent tableware for severe service conditions, Br. Ceram. Proc. 60 (1999) 347–348.
[23] W.M. Carty, U. Senapati, Porcelain-raw materials, processing, phase evolution, and mechanical behavior, J. Am. Ceram. Soc. 81 (1998) 3–20.
[24] P. Rado, The strange case of hard porcelain, Trans. Br. Ceram. Soc. 71 (1971) 131–139.
[25] S.I. Warshaw, R. Seider, Comparison of strength of triaxial porcelains containing alumina and silica, J. Am. Ceram. Soc. 50 (1967) 337–343.
[26] V.M.F. Marques, D.U. Tulyaganov, S. Agathopoulos, V.Kh. Gataullin, G.P. Kothiyal, J.M.F. Ferreira, Low temperature synthesis of anorthite based glass-ceramics via sintering and crystallization of glass-powder compacts, J. Eur. Ceram. Soc. 26 (2006) 2503–2510.
[27] H.L. Tang, J. Xua, H.J. Lia, Y.J. Dong, F. Wu, M.Q. Chen, Structure, thermal expansion and optical property of alumina-rich spinel substrate, J. Alloys Compd. 479 (2009) 26–29.
[28] Y. Kobayashi, M. Mukai, M. Nakayama, O. Ohira, H. Isoyama, Strength and thermal shock resistance of alumina-strengthened porcelain containing cristobalite, J. Ceram. Soc. Jpn. 111 (2003) 872–877.
[29] F. Bouzerara, A. Harabi, S. Achour, A. Larbot, Porous ceramic supports for membranes prepared from kaolin and doloma mixtures, J. Eur. Ceram. Soc. 26 (2006) 1663–1671.

[30] G.W. Brindley, M. Nakahira, The Kaolinite–Mullite reaction series: II. Metakaolin, J. Am. Ceram. Soc. 42 (1959) 314–318.
[31] I.A. Aksay, D.M. Dabbs, M. Sarikaya, Mullite for structural, electronic, and optical applications, J. Am. Ceram. Soc. 74 (1991) 2343.
[32] J.F. Li, H. Lin, J.B. Li, J. Wu, Effects of different potassium salts on the formation of mullite as the only crystal phase in kaolinite, J. Eur. Ceram. Soc. 29 (2009) 2929–2936.
[33] E.F. Osborn, A. Muan, System SiO_2–CaO–Al_2O_3. Phase equilibrium diagrams of oxide systems, Fig. 630, Am. Ceram. Soc. (1960).
[34] K. Traore, T.S. Kabre, P. Blanchart, Gehlenite and anorthite crystallisation from kaolinite and calcite mix, Ceram. Int. 29 (2003) 377–383.
[35] S.T. Lundin, Microstructure of porcelain (in microstructure of ceramic materials), NBS Mix. Publ. 257 (1964) 93–106.
[36] H.S. Kim, J.S. Choi, S.S. Kim, Physical and mechanical properties of roofing tiles produced in the Koryo and the Chosun dynasty, J. Kor. Anc. Histo. Soc. 32 (2000) 111–132.
[37] H.B. Poyraz, N. Erginel, N. Ay, The use of pumice in transparent roof tile glaze composition, J. Eur. Ceram. Soc. 26 (2006) 741–746.
[38] H. Kim, T. Kim, Measurement of hardness on traditional ceramics, J. Eur. Ceram. Soc. 22 (2002) 1437–1445.
[39] B.E. Yekta, P. Alizadeh, L. Rezazadeh, Floor tile glass–ceramic glaze for improvement of glaze surface properties, J. Eur. Ceram. Soc. 26 (2006) 3809–3812.
[40] M.F. Zawraha, E.M.A. Hamzawy, Effect of cristobalite formation on sinterability, microstructure and properties of glass/ceramic composites, Ceram. Int. 28 (2002) 123–130.
[41] R.C.Da Silva, S.A. Pianaro, S.M. Tebcherani, Preparation and characterization of glazes from combinations of different industrial wastes, Ceram. Int. (2011), doi:10.1016/j.ceramint. 2011.11.041.
[42] M. Llusar, C. Rodrigues, J. Labrincha, M. Flores, G. Monrós, Reinforcement of single-firing ceramic glazes with the addition of polycrystalline tetragonal zirconia (3Y-TZP) or zircon, J. Eur. Ceram. Soc. 22 (2002) 639–652.
[43] Y. Kobayashi, M. Mukai, T. Mizuno, O. Ohira, H. Isoyama, Effect of cristobalite formation and glaze on bending strength of a-alumina reinforced porcelain, J. Ceram. Soc. Jpn. 113 (2005) 413–418.